Electronic Supplementary Material (ESI) for Dalton Transactions.
This journal is © The Royal Society of Chemistry 2016

Supplementary Information

Coordination structure and extraction behavior of a silver ion with *N*-substituted-9-aza-3,6,12,15-tetrathiaheptadecanes: significant effect of Ph–C–N framework on the extractability

S. Iwatsuki,* A. Ichiyama, S. Tanooka, M. Toyama, K. Katagiri, M. Kawahata,
K. Yamaguchi, H. Danjo and K. Chayama*

Estimation procedure of K_{ex}^{pic}

The overall extraction equilibrium in the presence of an additional picrate ion (pic$^-$) at pH 6 (cf. Fig. 5c) is expressed as eqn S1:

$$Ag^+ + L_{org} + X^- \rightleftharpoons Ag(L)X_{org} \qquad (X = pic, CH_3COO, \text{ or } OH) \qquad (S1)$$

The apparent distribution ratio of Ag$^+$ (D_{Ag}') is expressed as eqn S2:

$$D_{Ag}' = \frac{[Ag(L)X]_{org}}{[Ag^+]} = \frac{[Ag(L)(pic)]_{org} + [Ag(L)(CH_3COO)]_{org} + [Ag(L)(OH)]_{org}}{[Ag^+]} \qquad (S2)$$

Since the distribution ratio (D_{Ag}^{abs}) in the absence of additional counter anions at pH 6 is expressed as eqn 7 in the text, the distribution ratio with respect to the extraction with pic$^-$ counter anion (D_{Ag}^{pic}) can be calculated by $D_{Ag}^{pic} = D_{Ag}' - D_{Ag}^{abs}$, where the D_{Ag}' and D_{Ag}^{abs} values were obtained from the data at pH 6 in Figs. 5c and 5a, respectively. By using the extraction constant $K_{ex}^{pic} = [Ag(L)(pic)]_{org}/([Ag^+][L]_{org}[pic^-])$, the D_{Ag}^{pic} is expressed as eqn S3:

$$D_{Ag}^{pic} = \frac{[Ag(L)(pic)]_{org}}{[Ag^+]} = K_{ex}^{pic}[L]_{org}[pic^-]$$

$$\log K_{ex}^{pic} = \log D_{Ag}^{pic} - \log[L]_{org} - \log[pic^-] \qquad (S3)$$

So the log K_{ex}^{pic} values for all extractant systems were calculated on the basis of eqn S3 from the D_{Ag}^{pic} values by using the values of $[L]_{org} \approx C_L = 5\times10^{-5}$ M and $[pic^-] \approx C_{pic} = 5\times10^{-5}$ M (because of C_L and $C_{pic} >> C_{Ag}$), and listed in Table 4.

Estimation procedure of K_{ex}^{OAc} and K_{ex}^{OH}

In the absence of additional counter anions, the possible counter monoanions at pH 6 (acetate buffer) for the Ag^+ extraction with L are CH_3COO^- and OH^-. The distribution ratio D_{Ag}^{abs} is expressed as eqn 7 in the text. Equation 7 can convert to a logarithmic equation S4 by using both extraction constants with CH_3COO^- and OH^- (K_{ex}^{OAc} = $[Ag(L)(CH_3COO)]_{org}/([Ag^+][L]_{org}[CH_3COO^-])$ and K_{ex}^{OH} = $[Ag(L)(CH_3COO)]_{org}([Ag^+][L]_{org}[OH^-]$, respectively):

$$\log D_{Ag}^{abs} = \log[L]_{org} + \log(K_{ex}^{OAc}[CH_3COO^-] + K_{ex}^{OH}[OH^-]) \qquad (S4)$$

Equation S4 indicates that the dependence of log D_{Ag}^{abs} on log $[CH_3COO^-]$ can be analyzed by nonlinear least-squares fitting under the conditions of $C_{Ag} << C_L$ at a constant pH, since $[L]_{org}$ and $[OH^-]$ are considered to be constant under these conditions. Fig. S6 shows the log D_{Ag}^{abs} vs. log $[CH_3COO^-]$ plots for the *N*-Bn-ATH and *N*-Ph_2CH-ATH systems at $C_{Ag} = 5\times10^{-5}$ M $<< C_L = 5\times10^{-5}$ M $\approx [L]_{org}$, and pH 6 ($[OH^-] = 1\times10^{-8}$ M) adjusted by acetate buffer. In this figure, $[CH_3COO^-]$ at pH 6.0 was calculated from the buffer concentration using the reported $pK_a = 4.58$ of acetic acid.[S1] The fitting curves using eqn S4 in Fig. S6 for both systems are consistent with the experimental data, indicating the nonlinear least-squares analyses are valid. The log K_{ex}^{OAc} and log K_{ex}^{OH} values are listed in Table 4.

Ref. [S1] E. Dubler, U. K. Häring, K. H. Scheller, P. Baltzer, H. Sigel, *Inorg. Chem.* 1984, **23**, 3785–3792.

Table S1. Slope and intercept in Fig. 6, and log K_{ex}^{NO3}

L (substituent)	slope	intercept	log $K_{ex}^{NO3\ a}$
N-H-ATH	0.90±0.04	3.1±0.1	7.4±0.1
N-Bn-ATH	0.91±0.07	4.6±0.3	8.9±0.3
N-NO_2Bn-ATH	0.92±0.05	4.3±0.2	8.6±0.2
N-Ph_2CH-ATH	0.93±0.03	3.9±0.1	8.2±0.1

[a] Estimated from the equation: intercept = log $[L]_{org}$ + log K_{ex}^{NO3} (cf. eqn 8 in the text)

Table S2a. Crystal and experimental data of [Ag(*N*-Bn-ATH)](BF_4)

Chemical formula: $C_{19}H_{33}AgBF_4NS_4$
Formula weight = 598.38
$T = 200$ K
Crystal system: Monoclinic   Space group: $P2_1/c$
$a = 12.9763(18)$Å
$b = 13.0824(18)$Å $\beta = 94.566(2)°$
$c = 15.111(2)$Å
$V = 2557.1(6)$Å^3 $Z = 4$
$D_x = 1.554$ g/cm^3
Radiation: Mo K_α ($\lambda = 0.71073$ Å)
μ(Mo K_α) = 1.151 mm^{-1} $F(000) = 1224$
Crystal size = 0.50 x 0.40 x 0.20 mm^3
No. of reflections collected = 11172
No. of independent reflections = 4396 [R(int) = 0.0228]
θ range for data collection: 2.06 to 24.78°
Data/Restraints/Parameters = 4396/0/300
Goodness-of-fit on F^2 = 1.070
R indices [$I > 2\sigma(I)$]: $R1 = 0.0316$, $wR2 = 0.0709$
R indices (all data): $R1 = 0.0422$, $wR2 = 0.0760$
$(\Delta/\sigma)_{max} = 0.001$
$(\Delta\rho)_{max} = 0.468$ eÅ^{-3} $(\Delta\rho)_{min} = -0.391$ eÅ^{-3}
Measurement: Bruker APEX II CCD Area Detector
Program system: Olex2
Structure determination: direct method (ShelXT-2015)
Refinement: full matrix least-squares on F^2 (ShelXL-2015)
CCDC deposition number: 1026848

Table S2b. Crystal and experimental data of [Ag(N-Ph$_2$CH-ATH)](BF$_4$)

Chemical formula: $C_{25}H_{37}AgBF_4NS_4$	
Formula weight = 674.48	
T = 173 K	
Crystal system: Triclinic	Space group: $P\overline{1}$
a = 8.7519(5)Å	α = 74.344(4)°
b = 10.4885(5)Å	β = 88.806(4)°
c = 16.6546(8)Å	γ = 81.965(4)°
V = 1457.40(13)Å^3	Z = 2
D_x = 1.555 g/cm^3	
Radiation: Cu K_α (λ = 1.54184 Å)	
μ(Cu K_α) = 8.606 mm^{-1}	F(000) = 700
Crystal size = 0.15 x 0.07 x 0.03 mm^3	
No. of reflections collected = 13332	
No. of independent reflections = 5618 [R(int) = 0.0456]	
θ range for data collection: 4.421 to 75.007°	
Data/Restraints/Parameters = 5618/0/327	
Goodness-of-fit on F^2 = 1.064	
R indices [$I > 2\sigma(I)$]: $R1$ = 0.0494, $wR2$ = 0.1306	
R indices (all data): $R1$ = 0.0586, $wR2$ = 0.1381	
$(\Delta/\sigma)_{max}$ = 0.001	
$(\Delta\rho)_{max}$ = 1.242 eÅ^{-3}	$(\Delta\rho)_{min}$ = –0.486 eÅ^{-3}
Measurement: XtaLAB Pro	
Program system: Olex2	
Structure determination: direct method (ShelXT-2015)	
Refinement: full matrix least-squares on F^2 (ShelXL-2015)	
CCDC deposition number: 1485984	

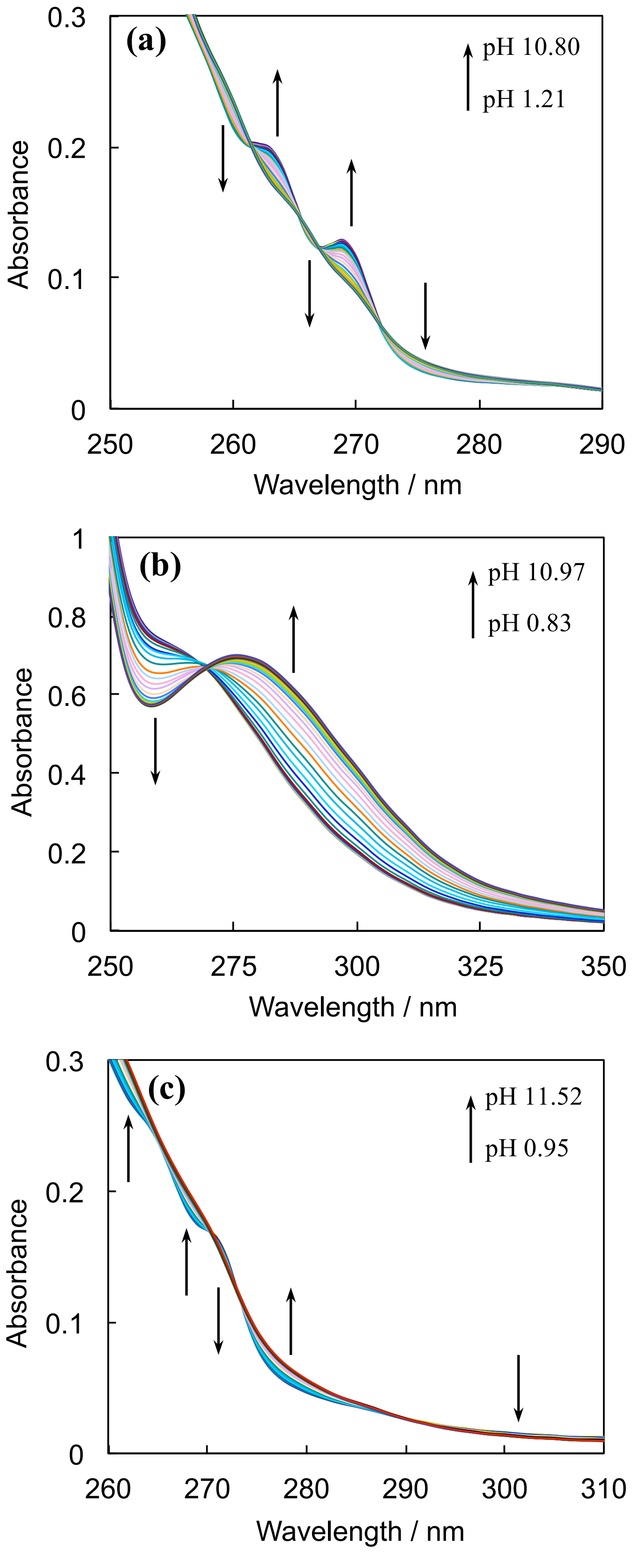

Fig. S1. UV-Vis spectra of (a) *N*-Bn-ATH (0.5 mM), (b) *N*-NO_2Bn-ATH (0.05 mM), and (c) *N*-Ph_2CH-ATH (0.2 mM) at various pH in 50v/v% 1,4-dioxane aqueous solution at 25ºC.

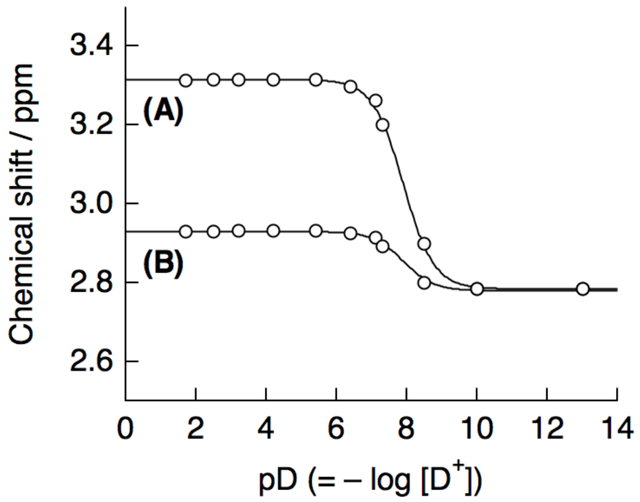

Fig. S2. The pD dependence of the ^{1}H NMR chemical shifts of *N*-H-ATH in 50v/v% 1,4-dioxane-d_8 in D_2O at 24°C. Chemical shifts (A) and (B) correspond to the $NC\underline{H}_2$ and $NCH_2C\underline{H}_2S$ protons, respectively. Internal reference: tetramethylammonium perchlorate (δ 3.19 ppm).

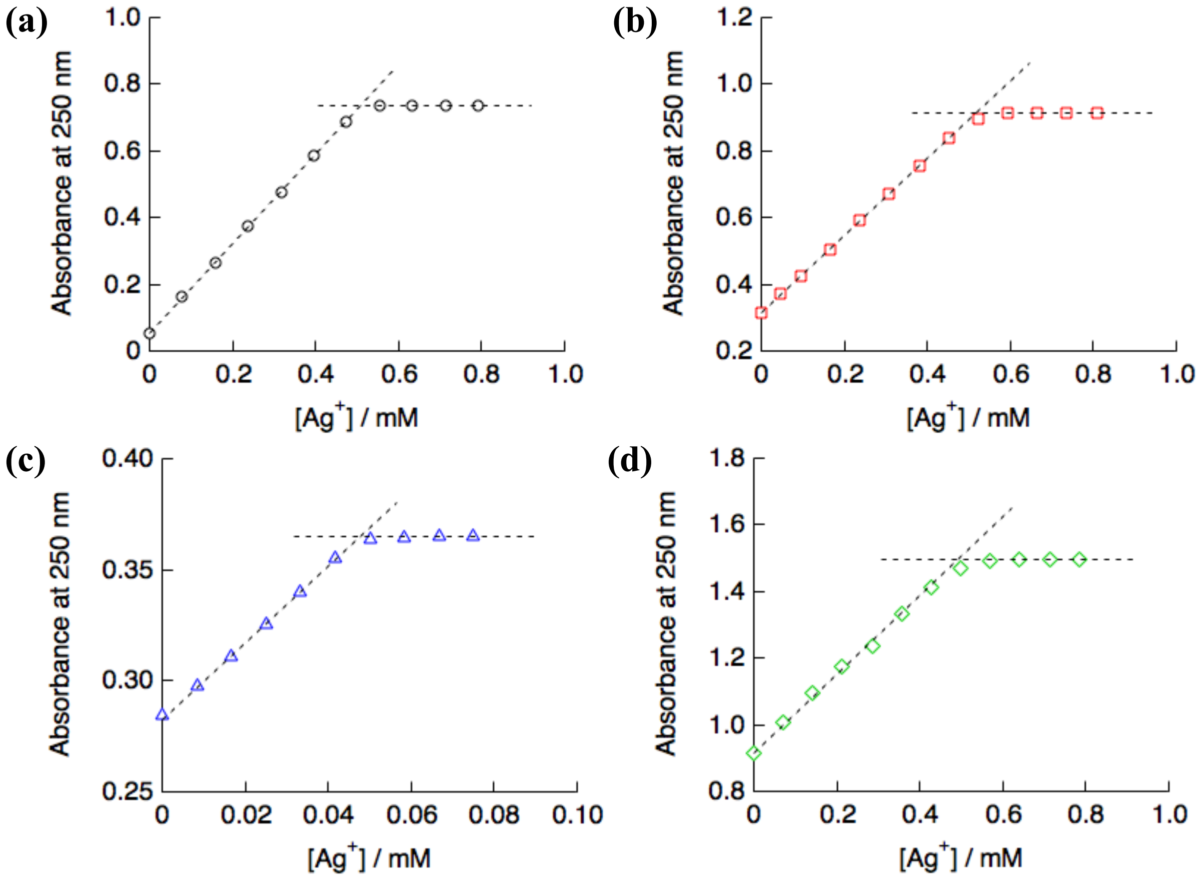

Fig. S3. The dependence of the absorbance at 250 nm of (a) *N*-H-ATH (0.5 mM), (b) *N*-Bn-ATH (0.5 mM), (c) *N*-NO_2Bn-ATH (0.05 mM), and (d) *N*-Ph_2CH-ATH (0.5 mM) on the $AgBF_4$ concentration in CH_3CN at 25°C. All bending points correspond to Ag^+:L = 1:1.

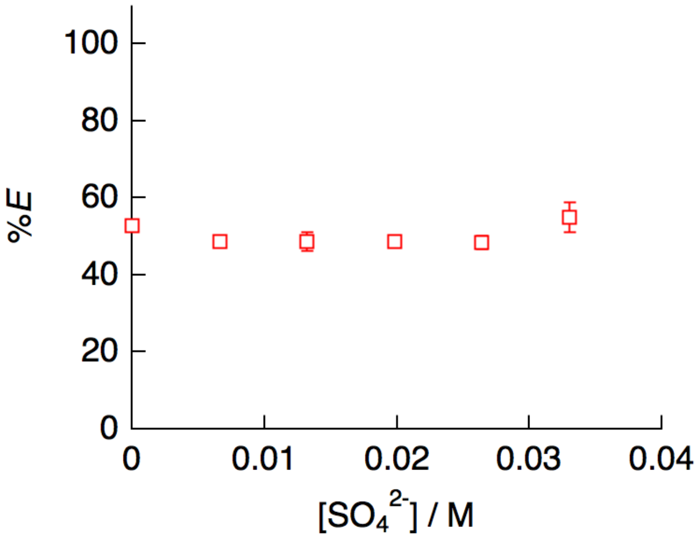

Fig. S4. The dependence of the Ag$^+$ extraction efficiency (%E) on the concentration of sulfate ion ([SO$_4^{2-}$]) for the N-Bn-ATH system. Initial concentration: $C_{\mathrm{Ag}} = 5.0\times10^{-6}$ M (pH 6.0 adjusted with 0.01 M of acetate buffer) in the aqueous phase, and $C_{\mathrm{L}} = 5.0\times10^{-5}$ M in the organic phase. At 25ºC.

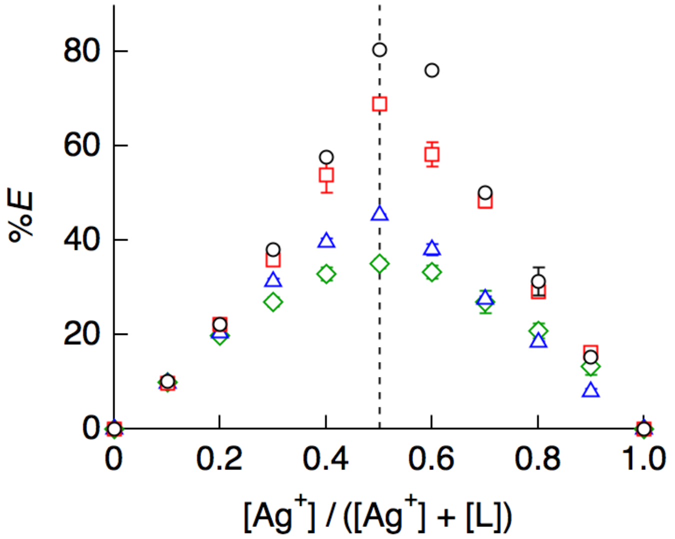

Fig. S5. Job's plots for the Ag$^+$ extraction with N-H-ATH (black circle), N-Bn-ATH (red square), N-NO$_2$Bn-ATH (blue triangle) and N-Ph$_2$CH-ATH (green diamond). A vertical broken line shows the concentration ratio of [Ag$^+$]:[L] = 1:1. Total concentration of Ag$^+$ and L: $C_{\mathrm{Ag}} + C_{\mathrm{L}} = 5.0\times10^{-6}$ M. The concentration of nitrate ion: 5.0×10^{-4} M for N-H-ATH system; 5.0×10^{-3} M for N-Bn-ATH system; 1.0×10^{-3} M for N-NO$_2$Bn-ATH and N-Ph$_2$CH-ATH systems. At pH = 6.0 (acetate buffer), I = 0.1 (Na$_2$SO$_4$), and 25ºC.

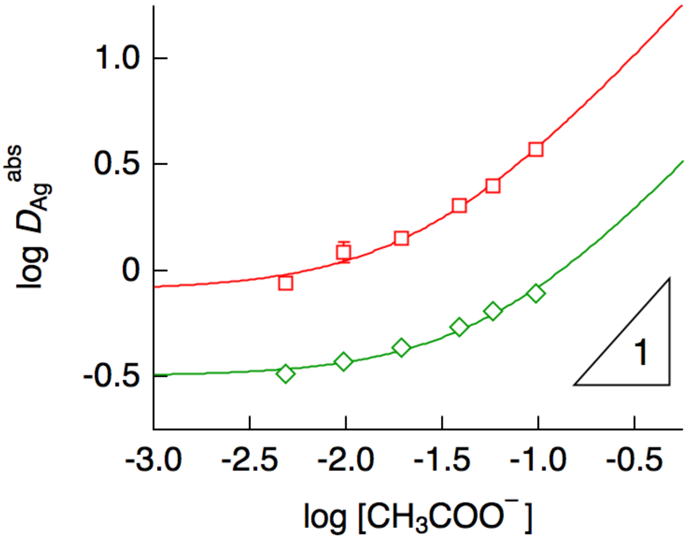

Fig. S6. The log D_{Ag}^{abs} vs. log [CH_3COO^-] plots for the Ag^+ extraction with *N*-Bn-ATH (red square) and *N*-Ph_2CH-ATH (green diamond) at pH 6.0 (acetate buffer). [CH_3COO^-] at pH 6.0 was calculated using the reported pK_a = 4.58 of acetic acid.[S1] The data are shown with best-fit curves based on eqn S4. Initial concentration: $C_{Ag} = 5.0\times10^{-6}$ M and $I = 0.1$ (Na_2SO_4) in aqueous phase, and $C_L = 5.0\times10^{-5}$ M in organic phase. At 25ºC.

Ref. [S1] E. Dubler, U. K. Häring, K. H. Scheller, P. Baltzer, H. Sigel, *Inorg. Chem.* 1984, **23**, 3785–3792.)

(a) [Ag(*N*-H-ATH)]$^+$ in CD_3CN

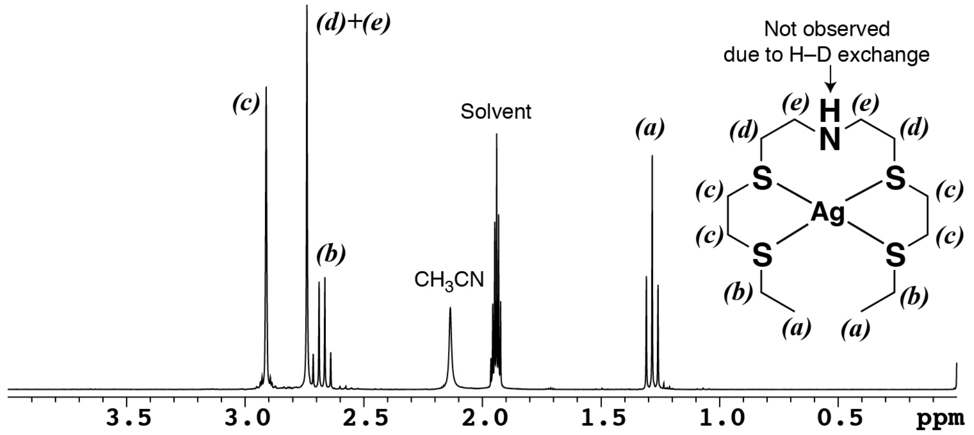

(b) [Ag(*N*-H-ATH)]$^+$ in CD_2Cl_2

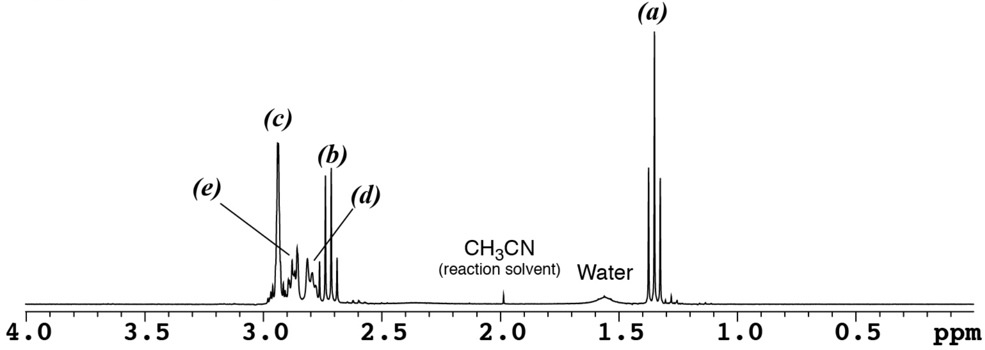

(c) [Ag(*N*-H-ATH)]$^+$ in CD_3OD

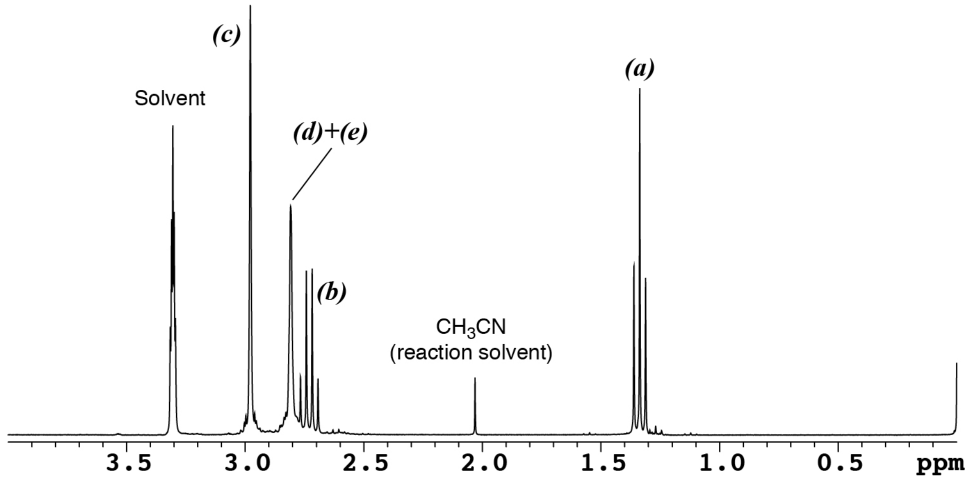

Fig. S7. The ^{1}H NMR spectra of [Ag(*N*-H-ATH)]$^+$ in CD_3CN (a), CD_2Cl_2 (b), and CD_3OD (c).

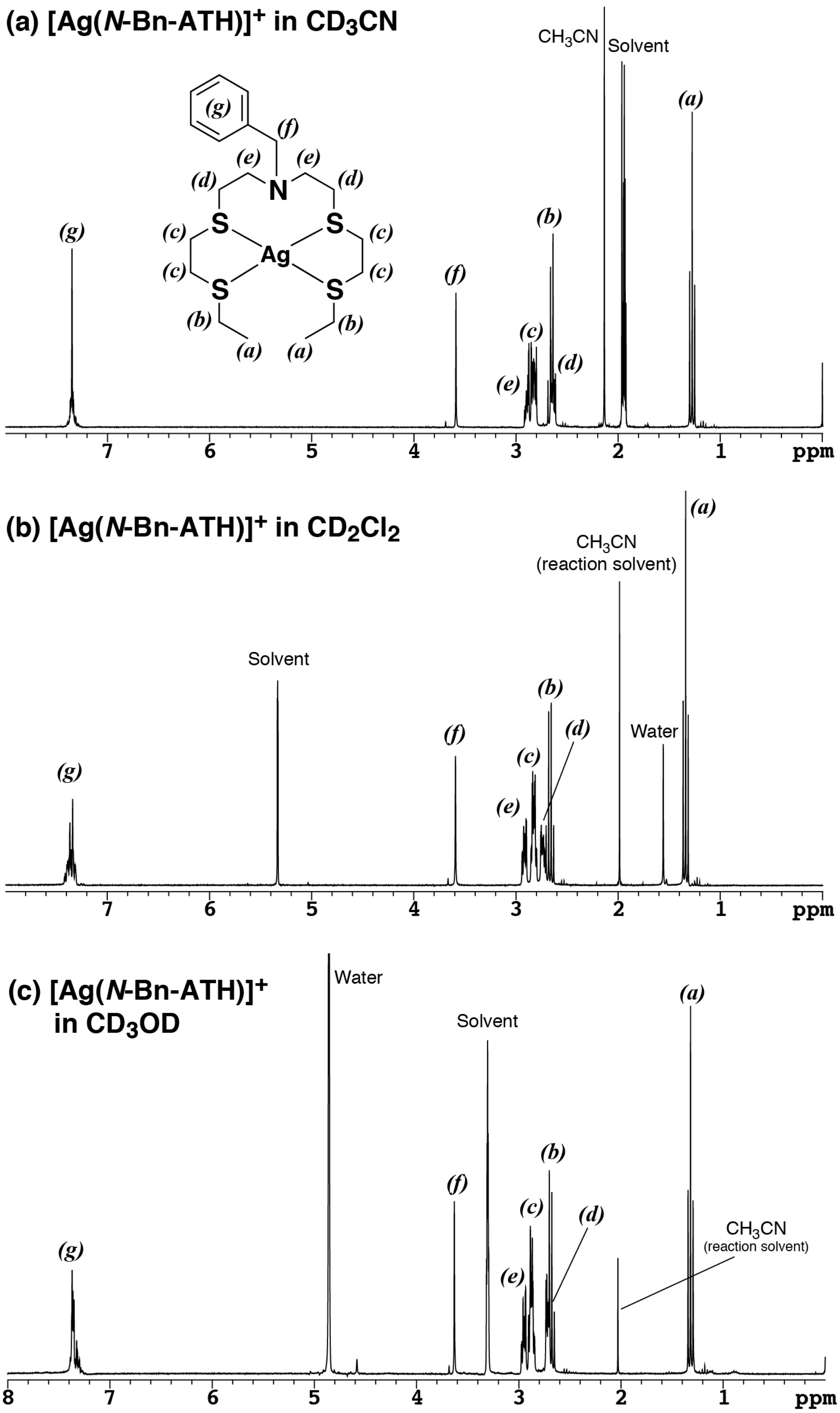

Fig. S8. The ^{1}H NMR spectra of [Ag(*N*-Bn-ATH)]$^+$ in CD_3CN (a), CD_2Cl_2 (b), and CD_3OD (c).

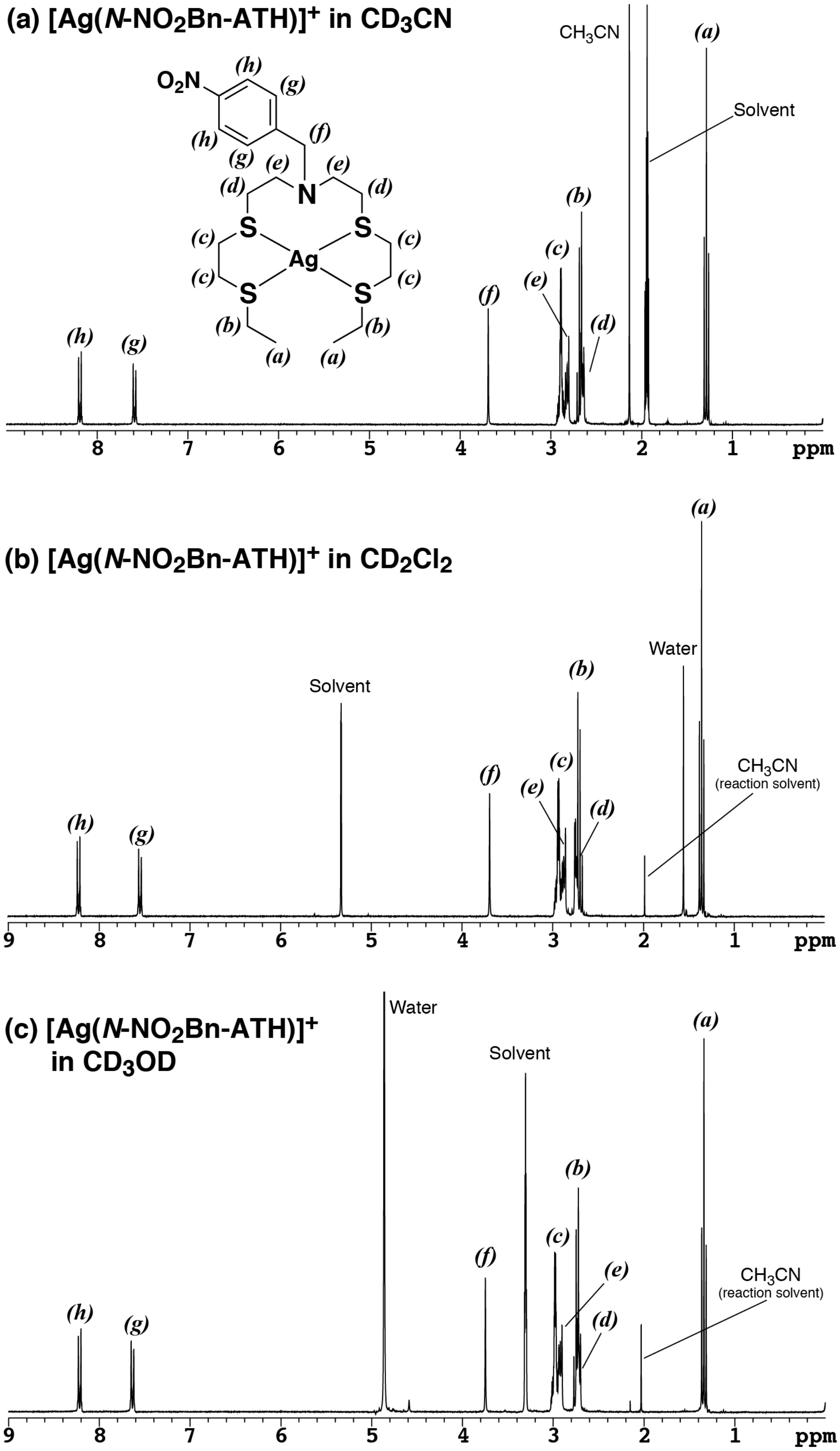

Fig. S9. The ^{1}H NMR spectra of $[Ag(N\text{-}NO_2Bn\text{-}ATH)]^+$ in CD_3CN (a), CD_2Cl_2 (b), and CD_3OD (c).

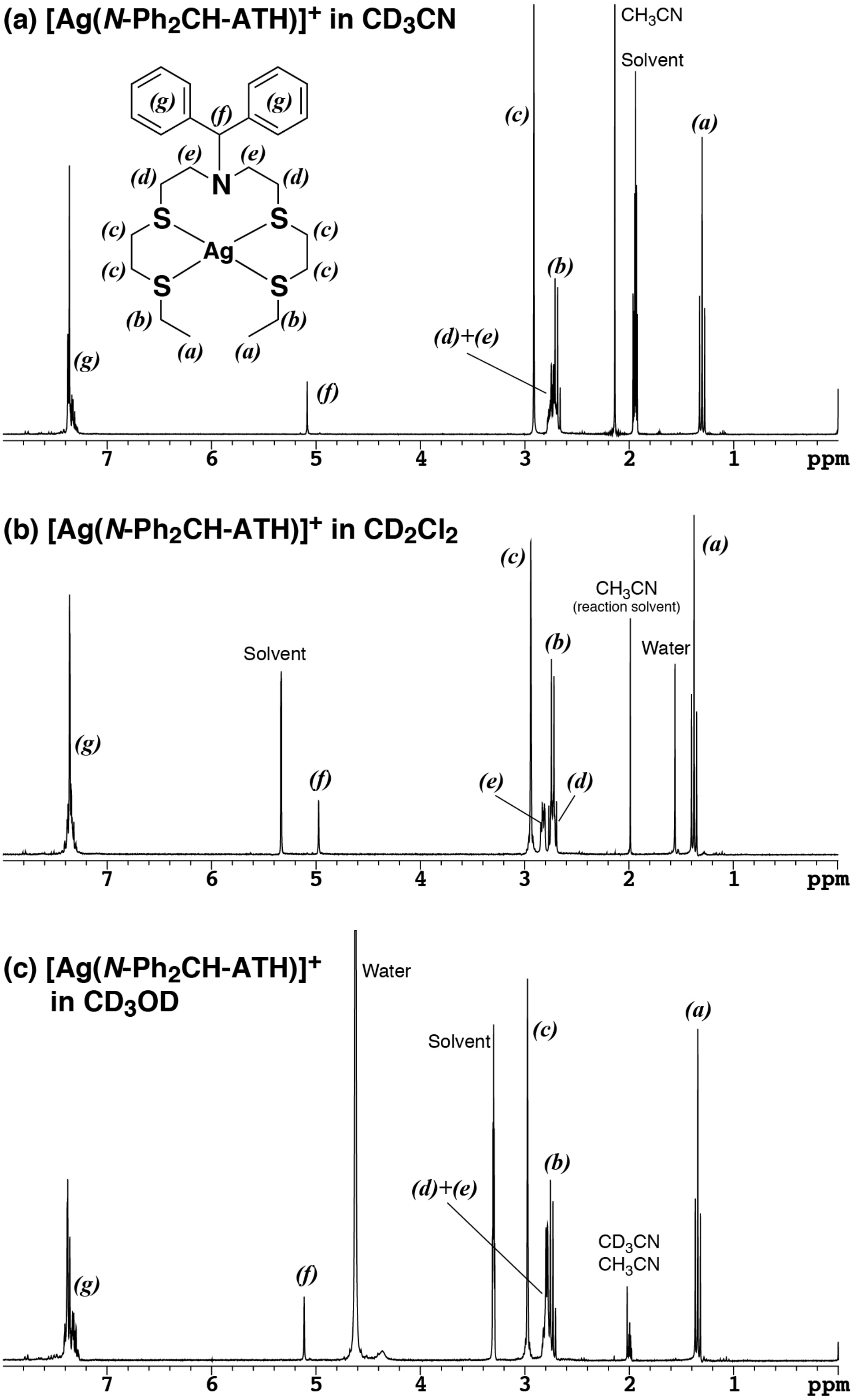

(a) $[Ag(N\text{-}Ph_2CH\text{-}ATH)]^+$ in CD_3CN

(b) $[Ag(N\text{-}Ph_2CH\text{-}ATH)]^+$ in CD_2Cl_2

(c) $[Ag(N\text{-}Ph_2CH\text{-}ATH)]^+$ in CD_3OD

Fig. S10. The ^1H NMR spectra of $[Ag(N\text{-}Ph_2CH\text{-}ATH)]^+$ in CD_3CN (a), CD_2Cl_2 (b), and CD_3OD containing 10v/v% CD_3CN (c).